Article:
Zhang, W. Q., Liu, Z., Andreyev, A. N. et al. (2026) Discovery of an Ipi=10+ Isomer in 150Yb: Nature of the Longest 10+ Isomeric Chain. Physical Review Letters. 082503. ISSN: 1079-7114

https://doi.org/10.1103/6cjc-bhfg

Discovery of an $I^\pi = 10^+$ isomer in ^{150}Yb: Nature of the longest 10^+ isomeric chain

W. Q. Zhang,[1] Z. Liu,[1,2,*] A. N. Andreyev,[3,†] Y. X. Yu,[4] G. J. Fu,[4,‡] C. Qi,[5] H. Huang,[1] X. H. Yu,[1,2] P. M. Walker,[6,§] X. H. Zhou,[1,2] P. T. Greenlees,[7] R. D. Page,[8] B. H. Sun,[9] S. F. Ashley,[10] I. G. Darby,[11] S. Eeckhaudt,[7] A. B. Garnsworthy,[12] M. B. Gómez-Hornillos,[13] T. Grahn,[7] D. G. Jenkins,[3] P. Jones,[14] R. Julin,[7] D. T. Joss,[8] S. Ketelhut,[7] J. G. Li,[1,2] M. Leino,[7] M. L. Liu,[15] Z. H. Li,[16] C. Ma,[17] M. Niikura,[18] M. Nyman,[19] J. Pakarinen,[7] S. Pietri,[20] Zs. Podolyák,[6] P. Rahkila,[7] J. Sarén,[7] N. J. Thompson,[6] J. Uusitalo,[7] T. Uesaka,[21] S. Williams,[6] Y. F. Wu,[1,2] X. X. Xu,[1,2] C. X. Yuan,[15] Q. B. Zeng,[1,2] F. S. Zhang,[22] and S. Y. Zhang[16]

[1] *State Key Laboratory of Heavy Ion Science and Technology, Institute of Modern Physics, Chinese Academy of Sciences, Lanzhou 730000, China*
[2] *University of Chinese Academy of Sciences, Beijing 100049, China*
[3] *School of Physics, Engineering and Technology, University of York, York, YO10 5DD, United Kingdom*
[4] *School of Physics Science and Engineering, Tongji University, Shanghai 200092, China*
[5] *KTH, Alba Nova University Center, SE-10691 Stockholm, Sweden*
[6] *Department of Physics, University of Surrey, Guildford GU2 7XH, United Kingdom*
[7] *Accelerator Laboratory, Department of Physics, University of Jyväskylä, FI-40014 Jyväskylä, Finland*
[8] *Department of Physics, Oliver Lodge Laboratory, University of Liverpool, Liverpool L69 7ZE, UK*
[9] *School of Physics and Nuclear Energy Engineering, Beihang University, Beijing 100191, China*
[10] *Sellafield Ltd, Seascale, Cumbria, CA20 1PG, United Kingdom*
[11] *Department of Nuclear Sciences and Applications, International Atomic Energy Agency, A-1400 Vienna, Austria*
[12] *TRIUMF, 4004 Wesbrook Mall, Vancouver, British Columbia V6T 2A3, Canada*
[13] *STFC, Daresbury Laboratory, Daresbury, Warrington, WA4 4AD, United Kingdom*
[14] *iThemba LABS, National Research Foundation, PO Box 722, Somerset West, South Africa*
[15] *Sino-French Institute of Nuclear Engineering and Technology, Sun Yat-sen University, Zhuhai 519082, China*
[16] *School of Physics and State Key Laboratory of Nuclear Physics and Technology, Peking University, Beijing 100871, China*
[17] *Shanghai Key Laboratory of Particle Physics and Cosmology, School of Physics and Astronomy, Shanghai Jiao Tong University, Shanghai 200240, China*
[18] *CNS, University of Tokyo, Tokyo 351-0100, Japan*
[19] *Department of Physics, University of Helsinki, FI-00014 Helsinki, Finland*
[20] *GSI Helmholtzzentrum für Schwerionenforschung, D-64291 Darmstadt, Germany*
[21] *RIKEN Nishina Center for Accelerator-Based Science, Saitama 351-0198, Japan*
[22] *The Key Laboratory of Beam Technology of Ministry of Education, College of Nuclear Science and Technology, Beijing Normal University, Beijing 100875, China*

(Dated: January 29, 2026)

Delayed γ-ray spectroscopy was performed for evaporation residues produced in the ^{58}Ni + ^{96}Ru reaction. A new isomer in $^{150}_{70}$Yb ($Z = 70$, $N = 80$) with a half-life of 0.62(5) μs was identified at an excitation energy of 2872(2) keV. Its spin-parity is assigned as (10^+) and a decay scheme is proposed based on a strong analogy with that of the isotonic $^{148}_{68}$Er. Previously, the 10^+ isomers were observed in the $N = 80$ even-Z isotones from the neutron-rich $^{126}_{46}$Pd to the neutron-deficient $^{148}_{68}$Er. For the first time, by combining experimental data and comprehensive large-scale shell-model calculations, we clearly identify the configurations of these isomers and demonstrate that they all exhibit seniority structures. These findings firmly establish a configuration change in the 10^+ isomeric chain, from a pair of maximally aligned $1h_{11/2}$ neutrons (holes) to a pair of maximally aligned $1h_{11/2}$ protons around the $Z = 64$ subshell closure. This transition serves as a unique isomeric relay underpinning the persistence of the isomeric chain.

The atomic nucleus exhibits shell structures for both protons and neutrons, characterized by the so-called magic numbers: Z, N = 2, 8, 20, 28, 50, 82, and N = 126. The stability of atomic nuclei, including both their ground and excited states, is strongly influenced by shell structures. In particular, specific excited states exhibit remarkably long lifetimes, making them not only promising for applications [1, 2], but also valuable probes of nuclear structure [3–6]. Such states are referred to as metastable states or isomers, based on a commonly used criterion of half-lives exceeding 10 ns, as adopted in the compilations of isomers [7, 8].

In the vicinity of magic nuclei, seniority isomers [9, 10] often appear, which arise from maximally aligned nucleons in high-j orbitals and are characterized by an approximately conserved seniority quantum number ν (the number of unpaired nucleons) [11–14]. Figure 1 illustrates the characteristic distribution of seniority isomers, by showing the occurrence of $I^\pi = 8^+$, 10^+, and 12^+ isomers in even-even nuclei throughout the nuclear chart. The majority of 8^+, 10^+, and 12^+ isomers are formed by a pair of nucleons occupying

$1g_{9/2}$, $1h_{11/2}$, and $1i_{13/2}$ orbitals, respectively, and exhibit seniority structure with $\nu = 2$. The three orbitals intrude into lower harmonic oscillator shells owing to spin-orbit coupling. Consequently, they possess much higher angular momentum and unique parity compared to other orbitals within the shell, rendering the corresponding maximally aligned configurations less susceptible to mixing. Therefore, seniority isomers offer a clear picture of nuclear structure and serve as sensitive probes of single-particle energy evolution [15].

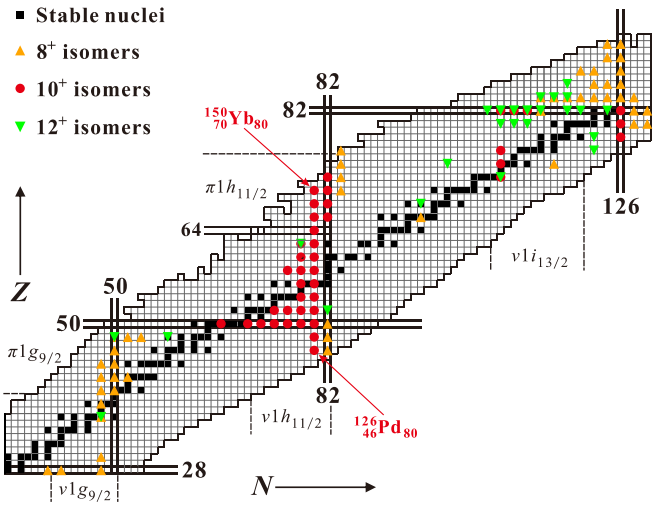

FIG. 1. Occurrence of 8^+, 10^+, and 12^+ isomers with half-lives > 10 ns in even-even nuclei on the partial nuclear chart. The dashed lines depict the approximate regions of high-j orbitals responsible for most of these isomers. The positions of magic numbers, including the $Z = 64$ subshell closure, are indicated by solid lines. The data are taken from Ref. [7, 16], and the present work for $^{150}_{70}$Yb.

In Fig. 1, the 10^+ isomeric chain in the $N = 80$ even-even isotones stands out, where an isomeric chain denotes a sequence of isomers with the same spin and parity along an isotopic or isotonic sequence. Previously, the 10^+ isomers had been reported from neutron-rich $^{126}_{46}$Pd up to neutron-deficient $^{148}_{68}$Er [7, 16], forming one of the longest continuous isomeric chains on the nuclear chart. The study in Ref. [15] showed that the 10^+ isomers in $^{126}_{46}$Pd and $^{128}_{48}$Cd have a two-neutron-hole configuration $\nu 1h^{-2}_{11/2}$, and play a pivotal role in probing single-neutron energy evolution below the $Z = 50$ shell closure. Above $Z = 50$, it was suggested in Refs. [17, 18] that, as the proton number increases, a configuration change from $\nu 1h^{-2}_{11/2}$ to $\pi 1h^{2}_{11/2}$ could occur for the 10^+ isomers around the $Z = 64$ subshell closure. While these studies provided pioneering insights into the changing nature of these isomers, a thorough analysis of the available experimental data and systematic theoretical calculations were missing.

Until now, the heaviest known member of this isomeric chain was the 10^+ isomer in $^{148}_{68}$Er discovered in 1982 [19]. The next $N = 80$, even-Z nuclide is $^{150}_{70}$Yb, the daughter nucleus of the first observed ground-state proton emitter $^{151}_{71}$Lu [20]. It was directly produced and identified in experiments at Michigan State University [21] and at TRIUMF [22], with the latter measuring its ground-state mass. Prior to the present work, no other spectroscopic information on $^{150}_{70}$Yb was available. On the theoretical front, calculations on excited states in $N = 80$ isotones have been performed only up to $^{142}_{62}$Sm [23–25].

In this Letter, we report the first observation of the long-sought 10^+ isomer in $^{150}_{70}$Yb, together with the first large-scale shell-model (LSSM) calculations for the $N = 80$ even-Z isotones $^{130}_{50}$Sn–$^{150}_{70}$Yb. These combined efforts allow us to elucidate the seniority structures of the 10^+ isomers in these isotones and to reveal the neutron-to-proton configuration transition. This change acts as an isomeric relay, handing over the long-lived isomerism from a neutron-dominated to a proton-dominated configuration while preserving the $1h_{11/2}$-based $\nu = 2$ seniority structure. No evidence for such relay behavior has been observed in any other isomeric chain.

The experiment was performed via delayed γ-ray spectroscopy at the gas-filled recoil separator RITU, located at the Accelerator Laboratory of the University of Jyväskylä (JYFL). A schematic view of the setup is shown in Fig. 1 of the Supplemental Material [26]. The ^{150}Yb nuclei were produced in the ^{96}Ru(^{58}Ni, $2p2n$)^{150}Yb fusion-evaporation reaction. The ^{58}Ni beam, at two energies of 266 and 274 MeV with an average current of 3 pnA, was delivered by the K130 cyclotron at JYFL for 110 hours. A self-supporting 500 μg/cm^2 ^{96}Ru target with an isotopic enrichment of $\sim 95\%$ was used. After a time of flight of ≈ 0.6 μs in RITU [29], the evaporation residues (ERs), including ^{150}Yb, passed through a multiwire proportional counter (MWPC) and were subsequently implanted into a pair of 300-μm thick double-sided silicon-strip detectors (DSSSDs) of the GREAT spectrometer [30]. The DSSSDs recorded signals of implanted recoils and charged particles ($p/\alpha/\beta$) from subsequent decays. Delayed γ rays emitted from implanted ERs were detected by three Compton-suppressed Clover germanium detectors and a planar double-sided germanium-strip detector (PGD). The PGD offers significantly enhanced sensitivity to low-energy γ rays and X-rays compared to the Clover detectors [30, 31], and has proven crucial for observing low-energy transitions in previous delayed-γ spectroscopy studies [32, 33].

To identify the 10^+ isomer in ^{150}Yb and to establish its decay scheme, recoil-gated delayed γ-ray singles and γ–γ coincidences were analysed. In Fig. 2(a), three new γ rays at 637, 708, and 857 keV were observed and found to be in mutual coincidence (see Fig. 2(b) as an example and Fig. 3 in the Supplemental Material [26]

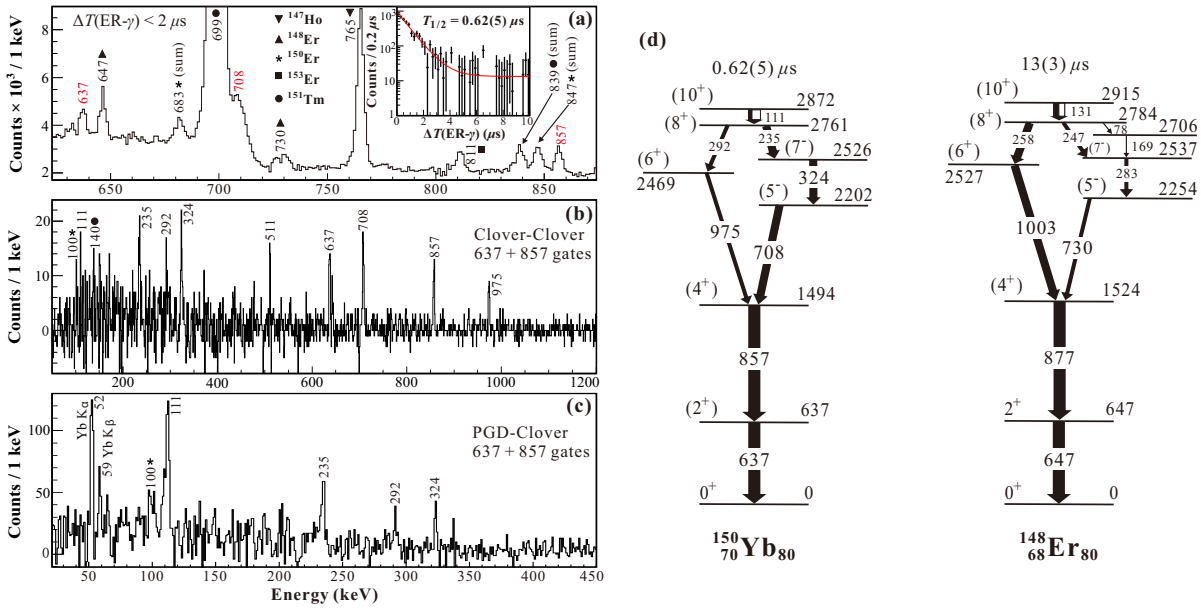

FIG. 2. (a) A portion of the recoil-gated delayed γ-ray singles spectrum registered in the Clover detectors within 2 μs after the ERs implantation, with the peaks labeled by transition energies and those from ^{150}Yb highlighted in red. The background from the $2 < \Delta T(\text{ER-}\gamma) < 4$ μs interval was subtracted to suppress prominent delayed γ rays originated from the microsecond isomers in $^{148-150}$Er and ^{151,152}Yb nuclei [16]. Peaks at 683, 839, and 847 keV are due to γ-ray summing effect. The presence of ^{153}Er reflects minor ^{96}Ru target contamination from heavier Ru isotopes. The inset shows the distribution of the time difference ΔT[ER-γ(637, 857 keV)] with a background subtraction performed by gating on nearby Compton background, and the associated fit by an exponential-plus-constant function. (b)–(c) The representative Clover-Clover and PGD-Clover γ–γ coincidence spectra. (d) The proposed decay scheme for the (10^+) isomer in ^{150}Yb and the decay scheme of the (10^+) isomer in the isotonic ^{148}Er [19]. The widths of arrows represent relative intensities of γ rays and internal conversion (white). Tentative spin-parity assignments are given in parentheses.

for details). As shown in Fig. 2(c), the 637- and 857-keV transitions are also coincident with several low-energy lines detected in the PGD, including the 111-, 235-, 292-, and 324-keV γ rays, and additionally with characteristic $K_{\alpha,\beta}$ X-rays of ytterbium. The last of these confirms that these γ rays originate from an isomer in an Yb isotope. Given that extensive studies of ^{151,152}Yb [34–36] have not found such an isomer, and that ^{149}Yb is expected to have a negligible production yield at the present beam energies according to the HIVAP calculations [37] (see Table I in the Supplemental Material [26]), the isomer is unambiguously assigned to ^{150}Yb.

Based on a strong similarity with the decay scheme of the (10^+) isomer in the isotone ^{148}Er [19], we assign a spin-parity of (10^+) and propose the decay scheme of the ^{150}Yb isomer, as illustrated in Fig. 2(d). The half-life $T_{1/2}(10^+) = 0.62(5)$ μs was derived from the time distribution ΔT[ER-γ(637, 857 keV)], as displayed in the inset of Fig. 2(a). The γ-ray energies and the relative intensities normalized to the 637-keV γ ray are summarized in Table I. On the basis of the analysis of γ-ray intensity balance and internal conversion coefficients provided in the Supplemental Material [26], the multipolarity of the 111-keV transition is inferred to be $E2$, resulting in a reduced transition probability [38] $B(E2) = 0.36(3)$ W.u. This value is much larger than the $B(E2; 10^+ \to 8^+)$ value of 0.012(3) W.u. in ^{148}Er [19], leading to the much shorter half-life of the (10^+) isomer in ^{150}Yb. A detailed discussion of the $B(E2)$ systematics will be presented in a follow-up paper [39].

TABLE I. Properties of the transitions deexciting the (10^+) isomer in ^{150}Yb.

E_x (keV)	E_γ (keV)	I_γ (%)	Transition $(J_i^\pi \to J_f^\pi)$
637.1(3)	637.1(3)	100(8)	$(2^+) \to 0^+$
1493.9(5)	856.8(4)	95(6)	$(4^+) \to (2^+)$
2202.1(6)	708.2(4)	70(14)	$(5^-) \to (4^+)$
2469(1)	975(1)	34(10)	$(6^+) \to (4^+)$
2526(1)	324(1)	66(15)	$(7^-) \to (5^-)$
2761(2)	235(1)	60(14)	$(8^+) \to (7^-)$
	292(1)	32(18)	$(8^+) \to (6^+)$
2872(2)	111(1)	30(11)	$(10^+) \to (8^+)$

To elucidate the nature of the 10^+ isomers in the $N = 80$ even-Z isotones and to comprehensively demonstrate the neutron-to-proton configuration transition, LSSM calculations have been performed. The calculations were

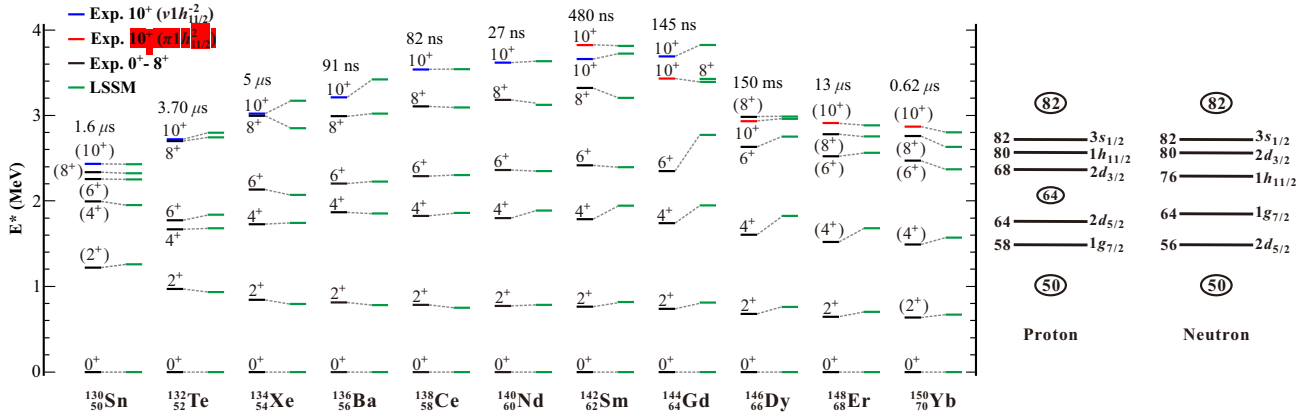

FIG. 3. The experimental low-lying positive-parity states of even-even $^{130}_{50}$Sn–$^{150}_{70}$Yb (taken from [16] and in this work) and the results of the LSSM calculations. Two types of 10^+ states are distinguished by color, corresponding to neutron- and proton-dominated configurations (see text). The half-lives of the 10^+_1 isomers are shown above the corresponding level schemes. In the rightmost, the orbitals between the $N(Z) = 50$–82 shell is shown. Note that according to the Fermi surface in the $A =$130–150 region, the $1h_{11/2}$, $2d_{3/2}$ and $3s_{1/2}$ orbitals lie relatively close in energy, and their ordering can change dynamically depending on the nucleon number.

carried out using the BIGSTICK code [40, 41] in a full major shell valence space between the magic numbers 50 and 82 for both protons and neutrons, comprising the $1g_{7/2}$, $2d_{5/2}$, $2d_{3/2}$, $3s_{1/2}$, and $1h_{11/2}$ orbitals outside an inert ^{100}Sn core. The effective interaction is a monopole- and multipole-optimized Hamiltonian derived from the realistic CD-Bonn [42] and JJ56PNA forces [43], which have been shown to successfully reproduce low-lying level structures in the $N = 81$ and 82 isotones [39, 44, 45]. More details regarding the calculations are provided in the Supplemental Material [26].

Figure 3 illustrates the overall agreement between experimental and calculated low-lying positive-parity states in the even-even $^{130}_{50}$Sn–$^{150}_{70}$Yb. These isotones have two-neutron holes with respect to the closed-shell $N = 82$ and increasing valence proton numbers outside the $Z = 50$ shell closure. This enables the formation of a 10^+ state by either a $1h_{11/2}$ neutron-hole pair or a $1h_{11/2}$ proton pair (except in $^{130}_{50}$Sn). Consequently, two distinct 10^+ states of neutron and proton origin are expected, and indeed two closely spaced 10^+ states have been observed in $^{142}_{62}$Sm and $^{144}_{64}$Gd (see Fig. 3), with the lower ones being 10^+_1 isomers while the 10^+_2 states decay promptly [16].

The Landé g-factors serve as sensitive probes for distinguishing the type of nucleons responsible for the configurations, by comparing with the Schmidt values [46]. In this work, the Schmidt values are calculated not only in the free-nucleon form but also with the standard quenching factor of 0.7 applied to the nucleon spin g-factor g_s, to account for the core polarization and in-medium effects [46, 47]. As shown in Fig. 4(a), the available experimental g-factors [48, 49] of the 10^+ states in $^{130}_{50}$Sn–$^{150}_{70}$Yb and those obtained from the LSSM are compared with the Schmidt values for the $1h_{11/2}$ neutron and proton.

In Fig. 4(a), the most salient feature predicted by the LSSM calculations is a clear separation of these 10^+ states into two distinct groups, with g-factor values close to -0.2 (Group A) for a neutron-based configuration and around $+1.2$ (Group B) for a proton-based one. The available experimental g-factor values confirm that the observed 10^+_1 states in $^{138}_{58}$Ce and $^{140}_{60}$Nd primarily originate from the coupling of two neutrons in the $1h_{11/2}$ orbital, whereas that in $^{144}_{64}$Gd is dominated by two $1h_{11/2}$ protons. The LSSM-predicted grouping is in agreement with these assignments. This consistency, together with the fact that the excitation energies of all these 10^+ states are well reproduced (Fig. 3), enables us to infer the underlying configurations of the remaining 10^+ states, even in the absence of measured g-factor values. Accordingly, the 10^+_1 isomers in $^{130}_{50}$Sn–$^{142}_{62}$Sm and the 10^+_2 states in $^{144}_{64}$Gd are assigned to Group A, while the 10^+_2 level in $^{142}_{62}$Sm and the 10^+_1 isomers in $^{144}_{64}$Gd–$^{150}_{70}$Yb belong to Group B. This classification clearly reveals an abrupt $\nu 1h^{-2}_{11/2} \rightarrow \pi 1h^{2}_{11/2}$ configuration change occurring around the $Z = 64$ subshell closure. Furthermore, both the experimental and LSSM g-factors agree remarkably well with the quenched Schmidt values, suggesting that these 10^+ states are largely unaffected by configuration mixing and retain a seniority character.

In addition to the g-factors, the LSSM calculations also provide the proton and neutron orbital occupancies for the two 10^+ groups, as shown in Fig. 4(b)–(c), offering further support for the configuration transition. The most pronounced difference between Groups A and B lies in the $\nu 1h_{11/2}$ hole occupancy (blue bars), which is close to 2 in Group A but nearly vanishes in Group B.

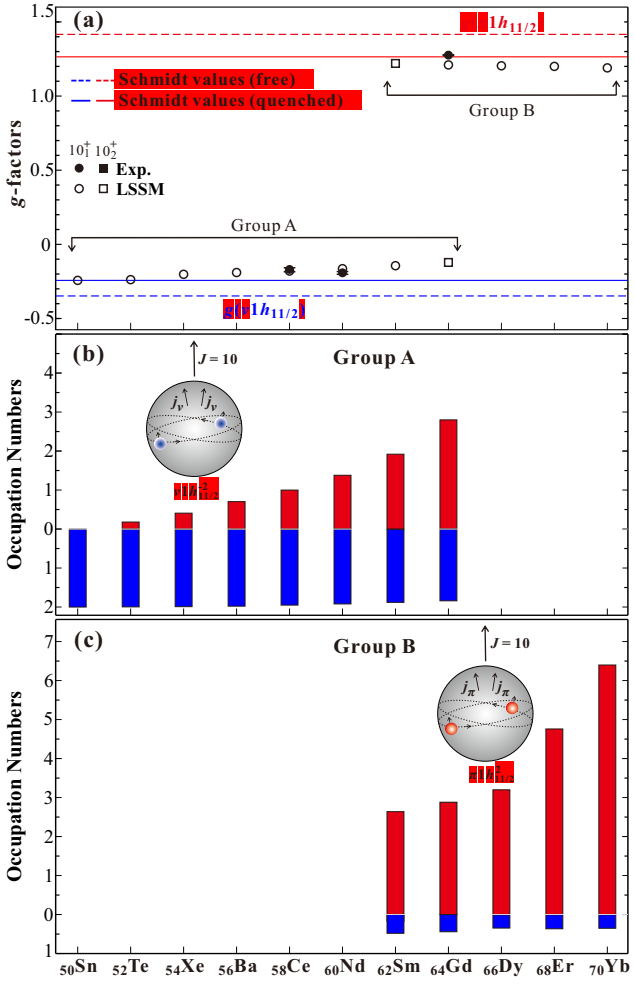

FIG. 4. (a) The g-factor data of the 10^+ states in the $N = 80$ even-Z isotones $^{130}_{50}$Sn–$^{150}_{70}$Yb. The available experimental g-factor data taken from [16, 48, 49] and the calculated values from the LSSM. The $g(\nu 1h_{11/2})$ and $g(\pi 1h_{11/2})$ denote the Schmidt values for the $1h_{11/2}$ neutron and proton, respectively. The dashed and solid lines correspond to the values calculated with free-nucleon and quenched g_s factors, respectively; see text for details. (b)–(c) The occupation numbers of the neutron hole $\nu 1h_{11/2}$ (blue, downwards) and proton $\pi 1h_{11/2}$ (red, upwards) orbitals for Groups A and B, respectively, with schematic illustrations of the $\nu 1h^{-2}_{11/2}$ and $\pi 1h^{2}_{11/2}$ couplings shown at the top of each panel.

This is fully in line with the two-neutron-hole $\nu 1h^{-2}_{11/2}$ configuration in the former and its absence in the latter. Moreover, the $\pi 1h_{11/2}$ particle occupancies (red bars) in Group B exceed 2 and increase with Z, supporting the two-proton-particle $\pi 1h^{2}_{11/2}$ configuration for this group.

These findings unveil that the persistence of the 10^+ isomeric chain in the $N = 80$ even-Z isotones arises from an isomeric relay, with the $\pi 1h^{2}_{11/2}$ configuration taking over the seniority isomerism from the $\nu 1h^{-2}_{11/2}$ configuration. As indicated by the single-particle level schemes shown at the rightmost side of Fig. 3, with increasing proton number, the proton Fermi surface gradually approaches the $\pi 1h_{11/2}$ orbital. This trend becomes particularly pronounced near the $Z = 64$ subshell closure, resulting in lower excitation energies of the proton 10^+ states. Simultaneously, in the neighboring $N = 81$ isotones, the energies of the $11/2^-$ levels dominated by $\nu 1h^{-1}_{11/2}$ rise as a manifestation of neutron shell evolution. This process is ascribed to the proton-neutron monopole interaction [50, 51], pushing up the neutron-hole 10^+ states [15]. These opposing trends drive the change from neutron to proton configuration in the 10^+ isomeric sequence taking place at $Z = 64$, thus making the 10^+ isomeric chain a unique laboratory for simultaneously tracing the evolution of both the proton and neutron $1h_{11/2}$ intruder orbitals.

These results have broader implications. The seniority structure exhibited by these 10^+ isomers supports that the $N = 82$ shell gap remains robust in this neutron-deficient region, as the presence of a seniority scheme is a good indicator of shell-gap stability [52]. Such a view is consistent with the conclusions of recent studies [22, 53] on the $N = 82$ shell-gap evolution towards the neutron-deficient side. The (10^+) isomer in $^{150}_{70}$Yb has a two-proton separation energy of $S_{2p} = -1138(45)$ keV [22, 54], rendering it an exceptionally rare seniority isomer built from a pair of unbound nucleons.

In conclusion, the long-sought (10^+) isomer in ^{150}Yb has been identified for the first time through delayed γ-ray spectroscopy at RITU. By combining experimental data with LSSM calculations, it is demonstrated that all 10^+ isomers in the $N = 80$ even-even isotones $^{130}_{50}$Sn–$^{150}_{70}$Yb exhibit seniority character. Furthermore, the neutron-to-proton configuration transition in the 10^+ isomeric chain has been firmly established, representing a unique isomeric relay that perpetuates this sequence. These findings support the robustness of the $N = 82$ shell gap in the neutron-deficient region. Further g-factor measurements of these 10^+ isomers would be important, especially for the 10^+ isomer in $^{142}_{62}$Sm, which could unambiguously determine the turning point of the neutron-to-proton configuration transition. The persistence of this isomeric chain suggests the existence of 10^+ isomers in more neutron-deficient isotones, such as $^{152}_{72}$Hf and $^{154}_{74}$W, thereby opening the possibility of the synthesis and identification of these yet-to-be-observed nuclei through delayed γ-ray spectroscopy.

Acknowledgments—We would like to thank the staff of the Accelerator Laboratory of the University of Jyväskylä for their support and dedicated efforts during the experimental campaign. The GAMMAPOOL European Spectroscopy Resource for the loan of the Clover Germanium detectors is acknowledged. We also acknowledge the support from High-Performance Computing platform at Tongji University. This

work has been supported by the National Natural Science Foundation of China (Grants No. 12135004, No. 12405140, No. 11961141004, No. U2032138, No. 12322506, No. 12075169, No. 12535009 and No. 12475129), the Strategic Priority Research Program of Chinese Academy of Sciences (Grant No. XDB34000000), the National Key R&D Program of China (Contract No. 2018YFA0404402), the Fundamental Research Funds for the Central Universities (Grant No. 22120250299), the Natural Science Foundation of Gansu Province, China (Grant No. 24JRRA033). A. N. Andreyev acknowledges the support from the Chinese Academy of Sciences President's International Fellowship Initiative (Grant No. 2020VMA0017). This work was also supported by the STFC through grants No. ST/P004598/1, No. ST/V001027/1 and No. ST/Y000242/1.

References

* liuzhong@impcas.ac.cn
† andrei.andreyev@york.ac.uk
‡ gjfu@tongji.edu.cn
§ p.walker@surrey.ac.uk

[1] M. A. Prelas, C. L. Weaver, M. L. Watermann, E. D. Lukosi, R. J. Schott, and D. A. Wisniewski, Progress in Nuclear Energy **75**, 117 (2014).
[2] S. Kraemer, J. Moens, M. Athanasakis-Kaklamanakis, S. Bara, K. Beeks, P. Chhetri, K. Chrysalidis, A. Claessens, T. E. Cocolios, J. G. M. Correia, H. D. Witte, R. Ferrer, S. Geldhof, R. Heinke, N. Hosseini, M. Huyse, U. Köster, Y. Kudryavtsev, M. Laatiaoui, R. Lica, G. Magchiels, V. Manea, C. Merckling, L. M. C. Pereira, S. Raeder, T. Schumm, S. Sels, P. G. Thirolf, S. M. Tunhuma, P. Van Den Bergh, P. Van Duppen, A. Vantomme, M. Verlinde, R. Villarreal, and U. Wahl, Nature **617**, 706 (2023).
[3] P. Walker and G. Dracoulis, Nature **399**, 35 (1999).
[4] G. D. Dracoulis, P. M. Walker, and F. G. Kondev, Reports on Progress in Physics **79**, 076301 (2016).
[5] P. M. Walker and Z. Podolyák, "Nuclear isomers," in *Handbook of Nuclear Physics*, edited by I. Tanihata, H. Toki, and T. Kajino (Springer Nature Singapore, Singapore, 2023) pp. 487–523.
[6] Z. Podolyák and P. Walker, "Isomeric states in nuclei," (2025).
[7] S. Garg, B. Maheshwari, B. Singh, Y. Sun, A. Goel, and A. K. Jain, Atomic Data and Nuclear Data Tables **150**, 101546 (2023).
[8] A. K. Jain, B. Maheshwari, and A. Goel, *Nuclear Isomers: A Primer*, 1st ed., Physics and Astronomy (R0) (Springer Cham, 2021) pp. XV, 144, 6 b/w illustrations, 43 illustrations in colour. Published online: 10 July 2021.
[9] P. Van Isacker, Eur. Phys. J. Spec. Top. **233**, 921 (2024).
[10] A. de Shalit and I. Talmi, *Nuclear Shell Theory* (Academic Press, New York, 1963).
[11] B. Flowers, Physica **18**, 1101 (1952).
[12] G. Racah, Phys. Rev. **62**, 438 (1942).
[13] G. Racah, in *L. Farkas Memorial Volume*, edited by A. Farkas and E. P. Wigner (Research Council of Israel, Jerusalem, 1952) pp. 294–304.
[14] I. Talmi, Nuclear Physics A **172**, 1 (1971).
[15] H. Watanabe, G. Lorusso, S. Nishimura, T. Otsuka, K. Ogawa, Z. Y. Xu, T. Sumikama, P.-A. Söderström, P. Doornenbal, Z. Li, F. Browne, G. Gey, H. S. Jung, J. Taprogge, Z. Vajta, J. Wu, A. Yagi, H. Baba, G. Benzoni, K. Y. Chae, F. C. L. Crespi, N. Fukuda, R. Gernhäuser, N. Inabe, T. Isobe, A. Jungclaus, D. Kameda, G. D. Kim, Y. K. Kim, I. Kojouharov, F. G. Kondev, T. Kubo, N. Kurz, Y. K. Kwon, G. J. Lane, C.-B. Moon, A. Montaner-Pizá, K. Moschner, F. Naqvi, M. Niikura, H. Nishibata, D. Nishimura, A. Odahara, R. Orlandi, Z. Patel, Z. Podolyák, H. Sakurai, H. Schaffner, G. S. Simpson, K. Steiger, H. Suzuki, H. Takeda, A. Wendt, and K. Yoshinaga, Phys. Rev. Lett. **113**, 042502 (2014).
[16] National Nuclear Data Center, https://www.nndc.bnl.gov/nudat2.
[17] M. Lach, J. Styczen, R. Julin, M. Piiparinen, H. Beuscher, P. Kleinheinz, and J. Blomqvist, Z. Phys. A **319**, 235 (1984).
[18] J. J. Valiente-Dobón, P. H. Regan, C. Wheldon, C. Y. Wu, N. Yoshinaga, K. Higashiyama, J. F. Smith, D. Cline, R. S. Chakrawarthy, R. Chapman, M. Cromaz, P. Fallon, S. J. Freeman, A. Görgen, W. Gelletly, A. Hayes, H. Hua, S. D. Langdown, I. Y. Lee, X. Liang, A. O. Macchiavelli, C. J. Pearson, Z. Podolyák, G. Sletten, R. Teng, D. Ward, D. D. Warner, and A. D. Yamamoto, Phys. Rev. C **69**, 024316 (2004).
[19] E. Nolte, G. Colombo, S. Z. Gui, G. Korschinek, W. Schollmeier, P. Kubik, S. Gustavsson, R. Geier, and H. Morinaga, Z. Phys. A **306**, 211 (1982).
[20] S. Hofmann, W. Reisdorf, G. Münzenberg, F. P. Heßberger, J. R. H. Schneider, and P. Armbruster, Z. Phys. A **305**, 111 (1982).
[21] G. A. Souliotis, Physica Scripta **2000**, 153 (2000).
[22] S. Beck, B. Kootte, I. Dedes, T. Dickel, A. A. Kwiatkowski, E. M. Lykiardopoulou, W. R. Plaß, M. P. Reiter, C. Andreoiu, J. Bergmann, T. Brunner, D. Curien, J. Dilling, J. Dudek, E. Dunling, J. Flowerdew, A. Gaamouci, L. Graham, G. Gwinner, A. Jacobs, R. Klawitter, Y. Lan, E. Leistenschneider, N. Minkov, V. Monier, I. Mukul, S. F. Paul, C. Scheidenberger, R. I. Thompson, J. L. Tracy, M. Vansteenkiste, H.-L. Wang, M. E. Wieser, C. Will, and J. Yang, Phys. Rev. Lett. **127**, 112501 (2021).
[23] C. Ma, Y. X. Yu, X. Yin, G. J. Fu, and Y. M. Zhao, Phys. Rev. C **112**, 014323 (2025).
[24] M. Bao, H. Jiang, Y. M. Zhao, and A. Arima, Phys. Rev. C **101**, 014316 (2020).
[25] T. Alharbi, P. H. Regan, P. J. R. Mason, N. Mărginean, Z. Podolyák, A. M. Bruce, E. C. Simpson, A. Algora, N. Alazemi, R. Britton, M. R. Bunce, D. Bucurescu, N. Cooper, D. Deleanu, D. Filipescu, W. Gelletly, D. Ghiță, T. Glodariu, G. Ilie, S. Kisyov, J. Lintott, S. Lalkovski, S. Liddick, C. Mihai, K. Mulholland, R. Mărginean, A. Negret, M. Nakhostin, C. R. Nita, O. J. Roberts, S. Rice, J. F. Smith, L. Stroe, T. Sava, C. Townsley, E. Wilson, V. Werner, M. Zhekova, and N. V. Zamfir, Phys. Rev. C **87**, 014323 (2013).

[26] See Supplemental Material at [URL] for a schematic view of the experimental setup and details of the multipolarity assignments and the LSSM calculations, which includes Refs. [27-28].

[27] C.-H. Yu, J. C. Batchelder, C. R. Bingham, R. Grzywacz, K. Rykaczewski, K. S. Toth, Y. Akovali, C. Baktash, A. Galindo-Uribarri, T. N. Ginter, C. J. Gross, M. Karny, S. H. Kim, B. D. MacDonald, S. D. Paul, D. C. Radford, J. Szerypo, and W. Weintraub, Phys. Rev. C **58**, R3042 (1998).

[28] T. Kibédi, T.W. Burrows, M.B. Trzhaskovskaya, P.M. Davidson, and C.W. Nestor, Nucl. Instrum. Methods Phys. Res. A **589**, 202 (2008).

[29] M. Leino, J. Äystö, T. Enqvist, P. Heikkinen, A. Jokinen, M. Nurmia, A. Ostrowski, W. Trzaska, J. Uusitalo, K. Eskola, P. Armbruster, and V. Ninov, Nucl. Instrum. Methods Phys. Res., Sect. B **99**, 653 (1995), application of Accelerators in Research and Industry '94.

[30] R. Page, A. Andreyev, D. Appelbe, P. Butler, S. Freeman, P. Greenlees, R.-D. Herzberg, D. Jenkins, G. Jones, P. Jones, D. Joss, R. Julin, H. Kettunen, M. Leino, P. Rahkila, P. Regan, J. Simpson, J. Uusitalo, S. Vincent, and R. Wadsworth, Nucl. Instrum. Methods Phys. Res., Sect. B **204**, 634 (2003), 14th International Conference on Electromagnetic Isotope Separators and Techniques Related to their Applications.

[31] A. Andreyev, P. Butler, R. Page, D. Appelbe, G. Jones, D. Joss, R.-D. Herzberg, P. Regan, J. Simpson, and R. Wadsworth, Nucl. Instrum. Methods Phys. Res., Sect. A **533**, 422 (2004).

[32] I. Darby, R. Page, D. Joss, J. Simpson, L. Bianco, R. Cooper, S. Eeckhaudt, S. Ertürk, B. Gall, T. Grahn, P. Greenlees, B. Hadinia, P. Jones, D. Judson, R. Julin, S. Juutinen, S. Ketelhut, M. Leino, A.-P. Leppänen, M. Nyman, P. Rahkila, J. Sarén, C. Scholey, A. Steer, J. Uusitalo, and M. Venhart, Physics Letters B **695**, 78 (2011).

[33] S. A. Gillespie, A. N. Andreyev, M. A. Monthery, C. J. Barton, S. Antalic, K. Auranen, H. Badran, D. Cox, J. G. Cubiss, D. O'Donnell, T. Grahn, P. T. Greenlees, A. Herzan, E. Higgins, R. Julin, S. Juutinen, J. Klimo, J. Konki, M. Leino, M. Mallaburn, J. Pakarinen, P. Papadakis, J. Partanen, P. M. Prajapati, P. Rahkila, M. Sandzelius, C. Scholey, J. Sorri, S. Stolze, R. Urban, J. Uusitalo, M. Venhart, and F. Weaving, Phys. Rev. C **99**, 064310 (2019).

[34] R. Broda, P. J. Daly, J. McNeill, R. V. F. Janssens, and D. C. Radford, Z. Phys. A **327**, 403 (1987).

[35] D. Nisius, B. Fornal, I. G. Bearden, R. Broda, R. H. Mayer, Z. W. Grabowski, P. J. Daly, C. N. Davids, I. Ahmad, B. B. Back, K. Bindra, M. P. Carpenter, W. Chung, D. Henderson, R. G. Henry, R. V. F. Janssens, T. L. Khoo, T. Lauritsen, Y. Liang, F. Soramel, and A. V. Ramayya, Phys. Rev. C **47**, 1929 (1993).

[36] D. Nisius, R. V. F. Janssens, I. G. Bearden, R. H. Mayer, I. Ahmad, P. Bhattacharyya, B. Crowell, M. P. Carpenter, P. J. Daly, C. N. Davids, Z. W. Grabowski, D. J. Henderson, R. G. Henry, R. Hermann, T. L. Khoo, T. Lauritsen, H. T. Penttilä, L. Ciszewski, and C. T. Zhang, Phys. Rev. C **52**, 1355 (1995).

[37] A. Gavron, Phys. Rev. C **21**, 230 (1980).

[38] R. B. Firestone, Transactions of the American Nuclear Society **75** (1996).

[39] Y. X. Yu *et al.*, in preparation.

[40] C. W. Johnson, W. E. Ormand, and P. G. Krastev, Computer Physics Communications **184**, 2761 (2013).

[41] C. W. Johnson, W. E. Ormand, K. S. McElvain, and H. Shan, arXiv:1801.08432.

[42] C. Qi and Z. X. Xu, Phys. Rev. C **86**, 044323 (2012).

[43] B. Brown and W. Rae, Nuclear Data Sheets **120**, 115 (2014).

[44] Q. Y. Chen, Y. X. Yu, S. T. Guo, G. J. Fu, and Z. Z. Ren, Nuclear Physics Review **41**, 606 (2024).

[45] Y. X. Yu, Q. Y. Chen, C. Qi, and G. J. Fu, arXiv:2507.14506.

[46] A. Bohr and B. R. Mottelson, *Nuclear Structure, Volume I: Single-Particle Motion* (Benjamin, New York, 1969).

[47] I. Towner, Physics Reports **155**, 263 (1987).

[48] O. Häusser, P. Taras, W. Trautmann, D. Ward, T. K. Alexander, H. R. Andrews, B. Haas, and D. Horn, Phys. Rev. Lett. **42**, 1451 (1979).

[49] J. Merdinger, F. Beck, E. Bozek, T. Byrski, C. Gehringer, Y. Schutz, and J. Vivien, Nuclear Physics A **346**, 281 (1980).

[50] A. de Shalit and M. Goldhaber, Phys. Rev. **92**, 1211 (1953).

[51] T. Otsuka, A. Gade, O. Sorlin, T. Suzuki, and Y. Utsuno, Rev. Mod. Phys. **92**, 015002 (2020).

[52] D. W. Luo, J. Z. Zhang, Z. H. Li, Y. Y. Cheng, H. Hua, H. Watanabe, G. Lorusso, C. X. Yuan, S. Nishimura, H. Baba, G. Benzoni, F. Browne, K. Y. Chae, Z. Q. Chen, F. C. L. Crespi, P. Doornenbal, N. Fukuda, R. Gernhäuser, G. Gey, C. Y. Guo, N. Inabe, T. Isobe, D. X. Jiang, Y. Jin, H. S. Jung, A. Jungclaus, D. Kameda, G. D. Kim, Y. K. Kim, I. Kojouharov, F. G. Kondev, T. Kubo, N. Kurz, Y. K. Kwon, G. J. Lane, X. Q. Li, J. L. Lou, A. Montaner-Pizá, K. Moschner, F. Naqvi, L. Ni, M. Niikura, H. Nishibata, A. Odahara, R. Orlandi, Z. Patel, Z. Podolyák, H. Sakurai, H. Schaffner, G. S. Simpson, P.-A. Söderström, K. Steiger, T. Sumikama, H. Suzuki, H. Takeda, J. Taprogge, Z. Vajta, A. Wendt, H. Y. Wu, J. Wu, C. Xu, Z. Y. Xu, A. Yagi, Y. L. Ye, K. Yoshinaga, S. Q. Zhang, S. Y. Zhang, and Z. X. Zhou, Phys. Rev. Lett. **134**, 232502 (2025).

[53] H. B. Yang, Z. G. Gan, Y. J. Li, M. L. Liu, S. Y. Xu, C. Liu, M. M. Zhang, Z. Y. Zhang, M. H. Huang, C. X. Yuan, S. Y. Wang, L. Ma, J. G. Wang, X. C. Han, A. Rohilla, S. Q. Zuo, X. Xiao, X. B. Zhang, L. Zhu, Z. F. Yue, Y. L. Tian, Y. S. Wang, C. L. Yang, Z. Zhao, X. Y. Huang, Z. C. Li, L. C. Sun, J. Y. Wang, H. R. Yang, Z. W. Lu, W. Q. Yang, X. H. Zhou, W. X. Huang, N. Wang, S. G. Zhou, Z. Z. Ren, and H. S. Xu, Phys. Rev. Lett. **132**, 072502 (2024).

[54] W. J. Huang, M. Wang, F. G. Kondev, G. Audi, and S. Naimi, Chin. Phys. C **45**, 030002 (2021).